

# Collective Vibrational Quantum Coherence in a Molecular Liquid under Spontaneous Raman Scattering

Santiago Tarrago Velez, Anna Pogrebna, and Christophe Galland  
*École polytechnique fédérale de Lausanne (EPFL),  
Institut de Physique, CH-1015 Lausanne, Switzerland*

(Dated: May 4, 2021)

Stimulated Raman scattering is conventionally employed to probe vibrational dynamics by inducing a coherent oscillation within a molecular ensemble. In contrast, spontaneous Raman scattering is considered as an incoherent process because the scattered field lacks any predictable phase relationship with the incoming laser pulse. It raises questions about the nature of the quantum state of a molecular ensemble following spontaneous Stokes scattering: should it be described as a statistical mixture of vibrationally excited molecules, where collective coherence is absent? Here, we measure time-resolved Stokes–anti-Stokes two-photon coincidences on a molecular liquid and find that a coherent superposition of two collective vibrational modes from two isotopic sub-ensembles is generated under spontaneous Raman scattering. Our results confirm that a spatially extended vibrational coherence emerges when a single collective excitation is spontaneously scattered and detected in a single spatiotemporal mode.

*Introduction.*— Raman scattering was first reported in 1928 [1] and with the advent of laser sources it has become an essential tool for probing and understanding the vibrational structure of organic and inorganic matter. The vast majority of measurements performed by Raman spectroscopy are well described by a semi-classical model of light-matter interaction, where quantizing the vibrational modes is only needed to explain the intensity asymmetry between Stokes and anti-Stokes scattering. But more recently experiments have shown that spontaneous Raman scattering combined with time-correlated single photon counting can be used to evidence non-classical intensity correlations between light fields interacting with the same individual phonon mode in diamond crystals [2] and molecular hydrogen gas [3, 4], with potential uses for ultrafast quantum information processing [5–10], novel forms of spectroscopy [11, 12], and the generation of non-classical states of light [13, 14]. These experimental results have in turn spurred further theoretical developments to understand how the Raman process leads to correlations between the photon and phonon fields [15, 16], the role that is played by the experimental geometry [17], and the effects of coupling the Raman scatterer to a nanocavity [18–20]. Despite these recent advances in understanding quantum coherence in vibrational Raman scattering, most reference texts only take into account the coherence among different molecules that is created by a beat note between two incoming laser fields, as in Coherent Anti-Stokes Raman Scattering (CARS) [21]. Any form of coherence among different molecules following spontaneous Raman scattering in a dense molecular liquid is usually neglected, implicitly assuming that the resulting collective vibrational state is a statistical mixture of individually excited molecules [22, 23].

In this Letter, we illustrate how spontaneous Raman scattering can naturally generate a collective vibrational excitation whose state is a quantum superposition of a macroscopic number of individually excited molecules in the liquid phase. In contrast with crystals, where all

atoms in the lattice are equally bounded to their nearest neighbors, the vibration of a molecule in a liquid can in principle be localized down to a single unit, as would be the case in single molecule spectroscopy. When shining light on an ensemble of molecules, however, spontaneous Raman scattering can create an excitation coherently shared among all the molecules that overlaps with the laser field. Moreover, the spontaneously created vibrational excitation can also be in a superposition of two distinct vibrational frequencies. It may occur if the ensemble contains two species of molecules (or two internal modes in a same species) with slightly different vibrational frequencies, and under the condition that the laser pulse duration is short enough to prevent leakage in the environment of the frequency information encoded in the Stokes field.

We experimentally demonstrate this phenomenon with a liquid of CS<sub>2</sub> molecules at room temperature (Fig. 1). CS<sub>2</sub> has two dominant naturally occurring isotopic variations, CS<sub>2</sub><sup>32</sup> and CS<sub>2</sub><sup>32</sup>S<sup>34</sup>. The frequencies (i.e. Raman shifts) of the symmetric stretch mode for these two isotopes are 655.3 cm<sup>-1</sup> (19.645 THz) and 646.7 cm<sup>-1</sup> (19.387 THz), respectively [24]. The frequency difference (8.6 cm<sup>-1</sup> or 258 GHz) is about 10 times smaller than the bandwidth of a Fourier-transform 200 fs laser pulse centered around 700 nm wavelength in vacuum – corresponding to our experimental conditions. Consequently, the temporal resolution is sufficiently high so as to erase spectral information about which of the two sub-ensembles of molecules was vibrationally excited. In such a situation, the principles of quantum mechanics predict that, during spontaneous Raman scattering, an individual quantum of vibration should be excited as a quantum coherent superposition of the two sub-ensembles. Such a scheme has been theoretically analysed in the context of cavity optomechanics [25], where it was proposed as a way to demonstrate quantum entanglement between different modes of the same mechanical oscillator. Our measurements provide the experimental evidence for this phe-

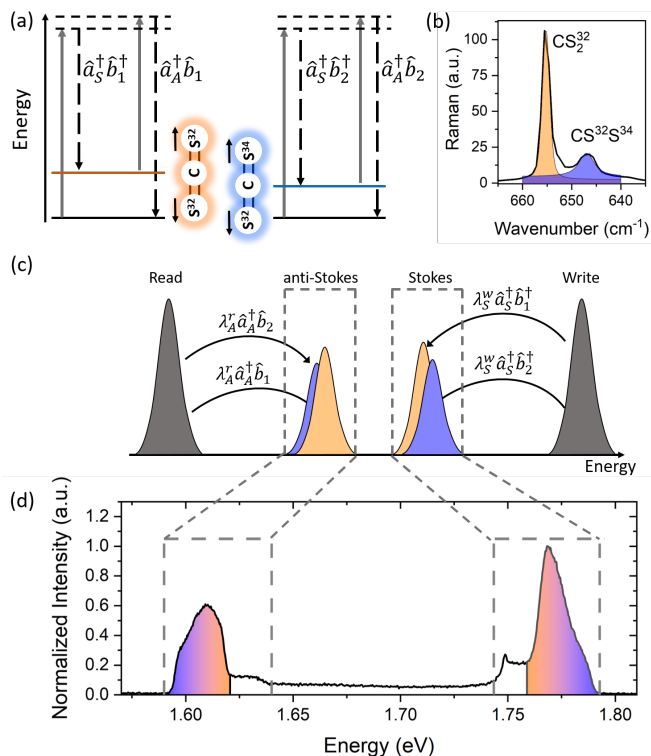


FIG. 1. Experimental concept. (a) Energy levels involved in Raman scattering, where the solid grey arrows represent the incoming radiation, while the dashed black arrows represent the inelastically scattered photons. (b) Raman spectrum of  $\text{CS}_2$  measured with a 785 nm cw laser. The Raman peaks around  $646 \text{ cm}^{-1}$  (shaded in orange) and  $655 \text{ cm}^{-1}$  (shaded in blue) are fitted with Voigt functions with relative area 1.00 and 0.50, respectively. (c) Frequency-domain schematic illustration of the signals detected in our experiment. (d) Stokes and anti-Stokes Raman spectra of carbon disulfide measured with 200 fs laser pulses with photon energy 1.85 eV and 1.53 eV, respectively. The Stokes signal is observed around 1.77 eV, while anti-Stokes at 1.62 eV. The Raman photons scattered by the two different isotopes are no longer distinguishable (graded shade). The spectral regions selected by filters before the single photon detectors are approximately marked by the dashed boxes.

nomenon, as supported by a full quantum model faithfully reproducing our results with photon noise as the only adjustable parameter.

*Experimental scheme.*—An experimental technique was introduced in [26] to measure the decay of a single phonon Fock state from time-correlated single photon counting on the Stokes and anti-Stokes fields generated by two non-degenerate sub-ps laser pulses. A first laser pulse generates a two-mode photon-phonon squeezed state via spontaneous Stokes Raman scattering. The power is adjusted to keep the probability of exciting a single phonon below  $\sim 10^{-2}$ , so that two-phonon processes have negligible impact on the measurement. A second laser pulse centered at a different wave-

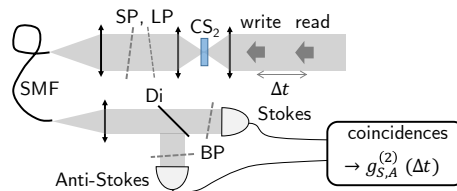


FIG. 2. Sketch of experimental setup. The liquid  $\text{CS}_2$  (anhydrous,  $\geq 99\%$ , Sigma Aldrich) is held between two objective lenses (numerical aperture: 0.8) in a quartz cuvette sealed with parafilm with 0.2 mm wall thickness and 1 mm optical path. The sample is studied in transmission to fulfill momentum conservation in the Stokes – anti-Stokes process mediated by a collective vibration with vanishing momentum. The Raman signal is collected into a single mode optical fiber (SMF), whose back-propagated image overlaps with the focused laser beams to define a single spatial mode inside the sample. After spatial filtering through the fiber, the Stokes and anti-Stokes photons from the first and second pulses, respectively, are separated based on their non-overlapping spectra (see Fig. 1d). Fiber-coupled single photon avalanche photodiodes are connected to a custom coincidence counter to measure  $g_{S,A}^{(2)}$ . SP: shortpass; LP: longpass; BP: bandpass; Di: dichroic.

length is used to probe the phonon mode occupancy after a variable time delay  $\Delta t$ . This information is encoded in the Stokes – anti-Stokes correlation function  $g_{S,A}^{(2)}(\Delta t)$  [27, 28]. The strength of phonon-mediated correlation is upper-bounded by  $g_{S,A}^{(2)} < 1 + 1/n_{th} \simeq 26$ , where the thermal occupancy of the vibrational mode is  $n_{th} \simeq 0.04$  in our system at room-temperature. A brief description of the experimental setup is provided in Fig. 2.

*Results.*— In Fig. 3 we show the normalised second order cross correlation function  $g_{S,A}^{(2)}$  measured on a liquid sample of  $\text{CS}_2$  with the technique described above, plotted as a function of time delay between Stokes and anti-Stokes processes. When write and read pulses are temporally overlapping, four-wave mixing (FWM) processes can generate photon pairs at any frequencies satisfying energy conservation, causing a rise in  $g_{S,A}^{(2)}$ . We found that using crossed-polarised laser pulses while filtering Raman photons co-polarised with the respective laser fields minimized the relative contribution of FWM to the overall signal – which is the configuration used here.

Information about the coherence and dynamics of the vibrational state is found at longer delays ( $\Delta t > 200$  fs). Assuming that spontaneous Raman scattering generates a statistical mixture of individually excited molecules, the expected decay is bi-exponential (because of the different linewidth of the two Raman peak, Fig. 1b), as shown by the dashed red line in Fig. 3. Instead, we observe oscillations with a period of around 3.7 ps (i.e. around  $9 \text{ cm}^{-1}$ ).

We note oscillations resulting from the excitation of vibrational modes in different isotopes of  $\text{CCl}_4$  [29] were observed using ultrafast stimulated Raman scattering in

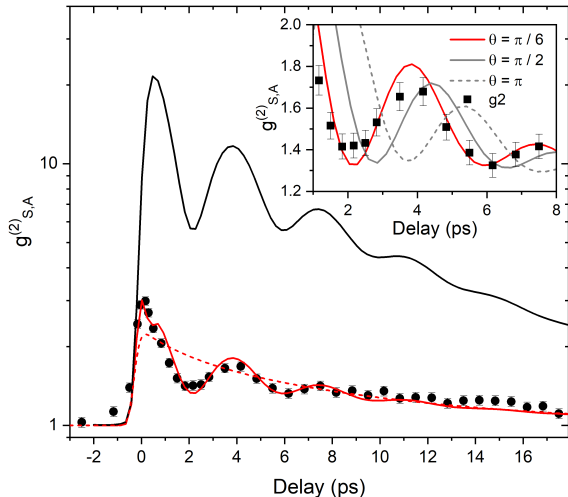


FIG. 3. Write-read delay dependence of the measured normalised Stokes-anti-Stokes correlations (full circles) and model prediction (solid lines), for  $\theta = \pi/6$ . The red line represents the prediction including noise, while the black line shows the ideal case without any detection noise but with thermal noise (see text). The dotted red line represents the bi-exponential decay that would be expected if the vibrational state were a statistical mixture of individually excited molecules. The inset shows the model predictions for different values of the phase  $\theta$ .

Ref. [30, 31]. However such experiments are well accounted for by a semi-classical model, in which the stimulated Stokes and anti-Stokes fields are classical. In the case of stimulated Raman scattering, the beating between the two pump laser fields is tuned resonant with the molecular vibration of interest, thereby driving a coherent collective vibration and resulting in a coherently oscillating Raman polarisation in the sample, all of which behave as classical variables.

In contrast, spontaneous Raman scattering and single photon counting demand a quantum description (detailed in the following section), in which the post-measurement vibrational state naturally appears as a quantum coherent superposition involving all molecules coupled to the light field. This quantum model makes predictions in good agreement with the data, after adjusting the relative contribution of FWM to fit the instantaneous response and taking into account detection noise. Moreover, the relative phase  $\theta$  that appears in the spontaneously generated quantum superposition of the two isotopic sub-ensembles translates into an horizontal shift of the oscillations. We find that taking  $\theta = \pi/6$  reproduces the position of the second oscillation peak. Our technique is therefore not only sensitive to the amplitudes in the quantum superposition but also to the relative phase.

*Theoretical description.*—The Raman interaction probabilistically generates a Stokes (resp. anti-Stokes) photon together with the creation (resp. annihilation) of a quantum of vibration. The two phonon modes of

interest in our experiment (for the two isotopic sub-ensembles) are described by the annihilation operators  $\hat{b}_1$ ,  $\hat{b}_2$ . The Raman signals from the two phonon modes can be spectrally distinguished under cw excitation, but become indistinguishable under pulsed excitation, as shown in Fig. 1. Therefore, in the pulsed experiment with single spatial mode filtering, both vibrational modes effectively couple to the same Stokes and anti-Stokes photon fields, described by the annihilation operators  $\hat{a}_S^x$ ,  $\hat{a}_A^x$ , where  $x = w, r$  for the write and read pulses, respectively. The Raman interaction is modeled by the Hamiltonian [32]

$$\hat{H}_I^x = \hbar\alpha^x \left[ \lambda_S^x (\hat{a}_S^x)^\dagger (\beta_1 \hat{b}_1^\dagger + e^{-i\theta_S^x} \beta_2 \hat{b}_2^\dagger) + \lambda_A^x (\hat{a}_A^x)^\dagger (\beta_1 \hat{b}_1 + e^{-i\theta_A^x} \beta_2 \hat{b}_2) \right] + h.c. \quad (1)$$

where the laser is modeled by a coherent field of amplitude  $\alpha_x(t)$  ( $x = w, r$ ) with Gaussian envelope centered at time  $t_{0x}$  of width  $\sigma_x$ ,

$$\alpha^x(t) = A_x \exp\left(\frac{(t - t_{0x})^2}{2\sigma_x^2}\right) \exp(-i\omega_x t). \quad (2)$$

In eq. (1)  $\lambda_{S,A}^x$  determine the coupling strengths to the Stokes and anti-Stokes modes, and  $\beta_1$ ,  $\beta_2$  control the relative weights of the two vibrational modes participating in the Raman interaction (experimentally related to the relative abundance and Raman cross-sections of the two main isotopic species), with  $\beta_1^2 + \beta_2^2 = 1$ . Since we use spectral filtering and post-selection to ignore events where an anti-Stokes (resp. Stokes) photon is emitted during the write (resp. read) pulse we can simplify the interaction model to

$$\hat{H}_I^w = \hbar\lambda_S^w \alpha^w (\hat{a}_S^w)^\dagger (\beta_1 \hat{b}_1^\dagger + e^{-i\theta_S^w} \beta_2 \hat{b}_2^\dagger) + h.c. \quad (3)$$

$$\hat{H}_I^r = \hbar\lambda_A^r \alpha^r (\hat{a}_A^r)^\dagger (\beta_1 \hat{b}_1 + e^{-i\theta_A^r} \beta_2 \hat{b}_2) + h.c. \quad (4)$$

(Note that the ignored terms contribute to uncorrelated noise photons generated via higher order Raman interactions during a single pulse [33].) We have explicitly written the two phase differences  $\theta_S^w$ , resp.  $\theta_A^r$ , appearing between the two vibrational modes during Stokes, resp. anti-Stokes, scattering. Our experiment is however only sensitive to their sum  $\theta = \theta_S^w + \theta_A^r$ . In the following we shorten the notation for the annihilation operators to  $\hat{a}_S^w \equiv \hat{a}_S$  and  $\hat{a}_A^r \equiv \hat{a}_A$ .

We include an additional  $\chi^{(3)}$  nonlinear interaction term that allows for the direct interaction between the write and read pulses, leading to the creation of photon pairs at the frequencies of the Stokes and anti-Stokes emission (FWM process):

$$\hat{H}_I^{(3)} = \hbar\lambda^{(3)} \alpha^w \alpha^r \hat{a}_S \hat{a}_A + h.c. \quad (5)$$

In the frame rotating with the central frequency  $\omega_0 = \frac{\omega_W + \omega_R}{2}$  we obtain the effective Hamiltonian

$$\hat{H} = \hbar\omega_1 \hat{b}_1^\dagger \hat{b}_1 + \hbar\omega_2 \hat{b}_2^\dagger \hat{b}_2 + \hbar\Delta_S \hat{a}_S^\dagger \hat{a}_S + \hbar\Delta_A \hat{a}_A^\dagger \hat{a}_A + \hat{H}_I^w + \hat{H}_I^r + \hat{H}_I^{(3)} \quad (6)$$

where  $\Delta_{S,A} = \omega_{S,A} - \omega_0$ . To account for dissipation we use the master equation approach, which includes coupling of the phonon modes to a thermal reservoir at room temperature, as described by the collapse operators

$$\begin{aligned}\hat{C}_{b1-} &= \sqrt{\kappa_1(1+n_{th})}\hat{b}_1 \\ \hat{C}_{b1+} &= \sqrt{\kappa_1 n_{th}}\hat{b}_1^\dagger \\ \hat{C}_{b2-} &= \sqrt{\kappa_2(1+n_{th})}\hat{b}_2 \\ \hat{C}_{b2+} &= \sqrt{\kappa_2 n_{th}}\hat{b}_2^\dagger\end{aligned}\quad (7)$$

where  $\kappa_x$  is related to the decay rate of the phonon modes by  $\tau_{ph_x} = 1/\kappa_x$ . The temporal evolution of the density matrix is computed numerically using QuTiP, an open-source library used for simulating quantum systems in Python [34, 35].

*Coincidence counts under non-ideal conditions.*— To account for noise and losses in the experiment we use the operator introduced in [36] to model the photon detection probability

$$\hat{D}_X = 1 - (1 - p_X^{dc})(1 - \eta_X)^{\hat{a}_X^\dagger \hat{a}_X} \quad (8)$$

where  $X = S, A$  for the Stokes and anti-Stokes detection channels, respectively. The dark count probability (per detection time window) is  $p_X^{dc}$  while  $\eta_X$  is the detection efficiency. The experimental value of the normalised Stokes – anti-Stokes coincidence rate  $g_{S,A}^{(2)}$  is then calculated (for several values of  $\Delta t = t_{0r} - t_{0w}$ ) as

$$g_{S,A}^{(2)} = \frac{\langle \hat{D}_S \hat{D}_A \rangle}{\langle \hat{D}_S \rangle \langle \hat{D}_A \rangle} \quad (9)$$

*Choice of model parameters.*— Most of the model parameters are extracted from the cw Raman spectra and the average single detector count rates during the experiment, leaving only the total phase  $\theta$  and the coupling strength of the FWM process  $\lambda^{(3)}$  as fitting parameters. We find the relation between the count rate in the cw experiment and the parameters  $\beta_1, \beta_2$ , by considering the state  $|\psi\rangle = \beta_1 |1\rangle_{b_1} \otimes |0\rangle_{b_2} + \beta_2 |0\rangle_{b_1} \otimes |1\rangle_{b_2}$ : Under cw excitation the photons scattered by the two vibrational modes are distinguishable, and their photon number is proportional to  $\beta_1^2$  and  $\beta_2^2$ . From the integrated area under the two main peaks in the cw spectrum shown in Fig. 1 we find approximately  $\beta_1 = \sqrt{1/3}$ ,  $\beta_2 = \sqrt{2/3}$ .

The detection efficiency of our setup is estimated to be  $\eta_S \approx \eta_A \approx 10\%$ . We fix the values of the parameters  $A_x$  and  $\lambda_{S,A}^x$  by considering the Stokes and anti-Stokes detection rates. As the pulse amplitudes  $A_x$  always appear in factor with the coupling rates  $\lambda^x$ , we introduce  $\Lambda_{S,A}^x = A_x \lambda_{S,A}^x$  whose values are chosen to reproduce the measured single-detector count rate when only the write or read pulse is propagating through the sample. We find  $\Lambda_S^w = 0.104$  and  $\Lambda_A^r = 0.136$ , which recover the measured detection probabilities  $p_S \approx 2.7 \times 10^{-4}$ ,  $p_A \approx 1.8 \times 10^{-5}$ . The dark count probabilities are estimated to be  $p_S^{dc} \approx 2 \times 10^{-4}$  and  $p_A^{dc} \approx 1 \times 10^{-5}$ .

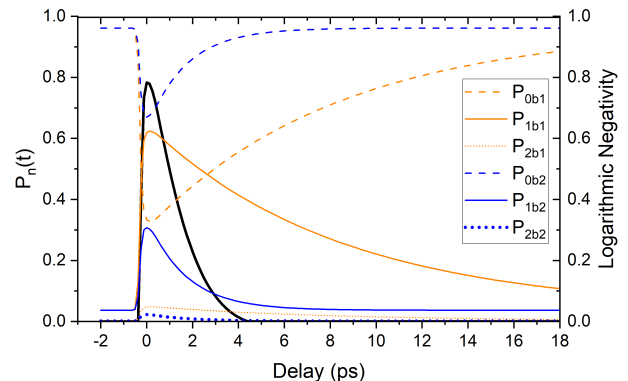


FIG. 4. Populations in the Fock state basis of the two vibrational modes (blue and orange lines) for the conditional state after heralding of a Stokes event, including all types of noises in the detection process (cf. red line in 3). The entanglement between the two vibrational modes in this heralded state is quantified by the Logarithmic Negativity  $E_N$ , shown as black solid line.

The coupling rates of the phonon modes to the thermal bath, which govern their decay times, is calculated from the FWHM  $\Delta\nu$  of each peak as measured by cw Raman spectroscopy. We fit the peaks with a Voigt function, which assumes a Lorentzian line shape for the peaks and a Gaussian response for the spectrometer, and use the FWHM of the Lorentzian curve to determine the lifetime of each phonon mode. The FWHM is related to the dephasing rate  $\Gamma$  of a phonon mode by  $\Gamma = \pi\Delta\nu$ . In the absence of pure dephasing, the phonon lifetime will be  $\tau_{ph} = 1/2\Gamma$ . We use this assumption to find  $\tau_{ph_1} = 8.4 \pm 1.3$  ps and  $\tau_{ph_2} = 1.7 \pm 0.2$  ps. With these parameters, the model outputs the full red line in Fig. 3, while the black line is the inferred signal in the absence of FWM and detection noise.

*Fock State Populations and Entanglement.*— As our model generates the full density matrix we can gain further insights into the dynamics and entanglement of the vibrational modes. We first compute the probabilities of observing different phonon numbers (Fock states) knowing that the Stokes detector registered a photon [2, 37], as a function of time after the Stokes scattering event; Fig. 4. Our evaluation includes the experimental noise, as we use the operator  $\hat{D}_S$  to model the detection of one or more Stokes photons; it can therefore be considered as a faithful estimate of the post-selected vibrational state in the experiment. Moreover, we can compute the amount of entanglement existing between the two vibrational modes, which we quantify via the Logarithmic Negativity  $E_N$ , an entanglement monotone defined by  $E_N = \log_2 \|\rho^{T_{b_2}}\|$ , where  $\rho^{T_{b_2}}$  indicates the partial transpose of  $\rho$  with respect to the phonon mode  $b_2$ , and  $\|X\| \equiv \text{tr}(\sqrt{X^\dagger X})$  [38, 39]. Fig. 4 shows that the two vibrational modes do become entangled ( $E_N > 0$ ), and that the entanglement survives for about 4.5 ps, decaying at a rate similar to that of  $\tau_{ph_2}$ , the faster decaying

phonon mode.

*Conclusions.*— To summarize, we presented a measurement of time domain spectrally resolved two-photon Stokes–anti-Stokes correlations on liquid CS<sub>2</sub> at room temperature. We showed that spontaneous Raman scattering from an ultrafast laser pulse creates a quantum superposition of two collective vibrational excitations of different isotopic sub-ensembles, which leads to quantum beats in the two-photon coincidence counts vs. time delay. Our experimental results are incompatible with the picture of spontaneous Raman scattering from a large ensemble as being the incoherent sum (statistical mixture) of single-molecule scattering events. As spontaneous Raman scattering has been considered an intrinsically incoherent process (e.g. [23]), our experiment nourishes the debate about the distinction between optical coherence and quantum coherence [40] and its relationship with entanglement [41], and it questions whether optical coher-

ent states are necessary to explain various forms of coherent spectroscopy. Finally, we note that our technique can be adapted to probe intramolecular vibrational entanglement and may inspire new forms of quantum-enhanced spectroscopy or have applications in ultrafast quantum information processing with dense molecular ensembles.

## ACKNOWLEDGEMENTS

The authors thank Vivishek Sudhir for insightful discussions and valuable comments. This work has received funding from the Swiss National Science Foundation (SNSF) (project no. PP00P2-170684) and the European Research Council’s (ERC) Horizon 2020 research and innovation programme (grant agreement no. 820196) A. P. acknowledges funding from the European Union’s Horizon 2020 research and innovation programme under the Marie Skłodowska-Curie grant agreement N° 754462.

- 
- [1] C. V. Raman and K. S. Krishnan, A new type of secondary radiation, *Nature* **121**, 501 (1928).
- [2] S. T. Velez, K. Seibold, N. Kipfer, M. D. Anderson, V. Sudhir, and C. Galland, Preparation and Decay of a Single Quantum of Vibration at Ambient Conditions, *Physical Review X* **9**, 41007 (2019).
- [3] P. J. Bustard, R. Lausten, D. G. England, and B. J. Sussman, Toward quantum processing in molecules: A thz-bandwidth coherent memory for light, *Physical review letters* **111**, 083901 (2013).
- [4] P. J. Bustard, J. Erskine, D. G. England, J. Nunn, P. Hockett, R. Lausten, M. Spanner, and B. J. Sussman, Nonclassical correlations between terahertz-bandwidth photons mediated by rotational quanta in hydrogen molecules, *Opt. Lett.*, OL **40**, 922 (2015).
- [5] K. C. Lee, B. J. Sussman, M. R. Sprague, P. Michelberger, K. F. Reim, J. Nunn, N. K. Langford, P. J. Bustard, D. Jaksch, and I. A. Walmsley, Macroscopic non-classical states and terahertz quantum processing in room-temperature diamond, *Nature Photonics* **6**, 41 (2012).
- [6] D. G. England, P. J. Bustard, J. Nunn, R. Lausten, and B. J. Sussman, From Photons to Phonons and Back: A THz Optical Memory in Diamond, *Phys. Rev. Lett.* **111**, 243601 (2013).
- [7] D. G. England, K. Fisher, J.-P. W. MacLean, P. J. Bustard, R. Lausten, K. J. Resch, and B. J. Sussman, Storage and Retrieval of THz-Bandwidth Single Photons Using a Room-Temperature Diamond Quantum Memory, *Phys. Rev. Lett.* **114**, 053602 (2015).
- [8] P.-Y. Hou, Y.-Y. Huang, X.-X. Yuan, X.-Y. Chang, C. Zu, L. He, and L.-M. Duan, Quantum teleportation from light beams to vibrational states of a macroscopic diamond, *Nat. Commun.* **7**, 11736 (2016).
- [9] K. A. Fisher, D. G. England, J. P. W. MacLean, P. J. Bustard, K. J. Resch, and B. J. Sussman, Frequency and bandwidth conversion of single photons in a room-temperature diamond quantum memory, *Nature Communications* **7**, 5 (2016).
- [10] K. A. G. Fisher, D. G. England, J.-P. W. MacLean, P. J. Bustard, K. Heshami, K. J. Resch, and B. J. Sussman, Storage of polarization-entangled THz-bandwidth photons in a diamond quantum memory, *Phys. Rev. A* **96**, 012324 (2017).
- [11] F. C. Waldermann, B. J. Sussman, J. Nunn, V. O. Lorenz, K. C. Lee, K. Surmacz, K. H. Lee, D. Jaksch, I. A. Walmsley, P. Spizziri, P. Olivero, and S. Praver, Measuring phonon dephasing with ultrafast pulses using Raman spectral interference, *Physical Review B* **78**, 155201 (2008).
- [12] S. Meiselman, O. Cohen, M. F. DeCamp, and V. O. Lorenz, Observation of coherence oscillations of single ensemble excitations in methanol, *Journal of the Optical Society of America B* **31**, 2131 (2014).
- [13] K. C. Lee, M. R. Sprague, B. J. Sussman, J. Nunn, N. K. Langford, X.-M. Jin, T. Champion, P. Michelberger, K. F. Reim, D. England, D. Jaksch, and I. A. Walmsley, Entangling Macroscopic Diamonds at Room Temperature, *Science* **334**, 1253 (2011).
- [14] S. T. Velez, V. Sudhir, N. Sangouard, and C. Galland, Bell correlations between light and vibration at ambient conditions, *Science Advances* **6**, eabb0260 (2020).
- [15] K. Thapliyal and J. Peřina Jr, Ideal pairing of the stokes and anti-stokes photons in the raman process, *Physical Review A* **103**, 033708 (2021).
- [16] R. A. Diaz, C. Monken, A. Jorio, and M. F. Santos, Effective hamiltonian for stokes–anti-stokes pair generation with pump and probe polarized modes, *Physical Review B* **102**, 134304 (2020).
- [17] K. Shinbrough, Y. Teng, B. Fang, V. O. Lorenz, and O. Cohen, Photon-matter quantum correlations in spontaneous raman scattering, *Physical Review A* **101**, 013415 (2020).
- [18] P. Roelli, C. Galland, N. Piro, and T. J. Kippenberg, Molecular cavity optomechanics as a theory of plasmon-enhanced Raman scattering, *Nat Nano* **11**, 164 (2016).
- [19] Y. Zhang, J. Aizpurua, and R. Esteban, Optomechanical collective effects in surface-enhanced raman scatter-

- ing from many molecules, *ACS Photonics* **7**, 1676 (2020), <https://doi.org/10.1021/acsp Photonics.0c00032>.
- [20] M. K. Schmidt, R. Esteban, G. Giedke, J. Aizpurua, and A. Gonzalez-Tudela, Frequency-resolved photon correlations in cavity optomechanics, *Quantum Science and Technology* (2021).
- [21] B. Schrader, *Infrared and Raman spectroscopy: methods and applications* (John Wiley & Sons, 2008).
- [22] D. A. Long, *The Raman effect: a unified treatment of the theory of Raman scattering by molecules* (Wiley, 2002).
- [23] E. Le Ru and P. Etchegoin, *Principles of Surface-Enhanced Raman Spectroscopy: and related plasmonic effects* (Elsevier, 2008).
- [24] M. Ito, Raman and infrared spectra of crystalline carbon disulfide, *The Journal of Chemical Physics* **42**, 815 (1965).
- [25] H. Flayac and V. Savona, Heralded preparation and readout of entangled phonons in a photonic crystal cavity, *Physical Review Letters* **113**, 1 (2014), arXiv:1407.5275.
- [26] M. D. Anderson, S. Tarrago Velez, K. Seibold, H. Flayac, V. Savona, N. Sangouard, and C. Galland, Two-Color Pump-Probe Measurement of Photonic Quantum Correlations Mediated by a Single Phonon, *Physical Review Letters* **120**, 233601 (2018).
- [27] C. Galland, N. Sangouard, N. Piro, N. Gisin, and T. J. Kippenberg, Heralded single-phonon preparation, storage, and readout in cavity optomechanics, *Phys. Rev. Lett.* **112**, 143602 (2014).
- [28] R. Riedinger, S. Hong, R. A. Norte, J. A. Slater, J. Shang, A. G. Krause, V. Anant, M. Aspelmeyer, and S. Gröblacher, Non-classical correlations between single photons and phonons from a mechanical oscillator, *Nature* **530**, 313 (2016).
- [29] C. K. Wu and G. B. M. Sutherland, The Isotope Effect in the Vibration Spectrum of CCl<sub>4</sub>, *The Journal of Chemical Physics* **6**, 114 (1938).
- [30] A. Laubereau, G. Wochner, and W. Kaiser, Collective beating of molecular vibrations in liquids on the picosecond time scale, *Optics Communications* **17**, 91 (1976).
- [31] J. Konarska, W. Gadomski, B. Ratajska-Gadomska, K. Polok, G. Pudłowski, and T. M. Kardaś, Dynamics of intermolecular interactions in CCl<sub>4</sub> via the isotope effect by femtosecond time-resolved spectroscopy, *Physical Chemistry Chemical Physics* **18**, 16046 (2016).
- [32] T. von Foerster and R. J. Glauber, Quantum theory of light propagation in amplifying media, *Phys. Rev. A* **3**, 1484 (1971).
- [33] C. A. Parra-Murillo, M. F. Santos, C. H. Monkens, and A. Jorio, Stokes–anti-stokes correlation in the inelastic scattering of light by matter and generalization of the bose-einstein population function, *Phys. Rev. B* **93**, 125141 (2016).
- [34] J. R. Johansson, P. D. Nation, and F. Nori, Qutip: An open-source python framework for the dynamics of open quantum systems, *Computer Physics Communications* **183**, 1760 (2012).
- [35] J. R. Johansson, P. D. Nation, and F. Nori, Qutip 2: A python framework for the dynamics of open quantum systems, *Comp. Phys. Comm* **184**, 1234 (2013).
- [36] P. Sekatski, N. Sangouard, F. Bussières, C. Clausen, N. Gisin, and H. Zbinden, Detector imperfections in photon-pair source characterization, *J. Phys. B At. Mol. Opt. Phys.* **45**, 124016 (2012).
- [37] S. Hong, R. Riedinger, I. Marinković, A. Wallucks, S. G. Hofer, R. A. Norte, M. Aspelmeyer, and S. Gröblacher, Hanbury brown and twiss interferometry of single phonons from an optomechanical resonator, *Science* **358**, 203 (2017).
- [38] G. Vidal and R. F. Werner, Computable measure of entanglement, *Physical Review A* **65**, 032314 (2002).
- [39] M. B. Plenio, Logarithmic negativity: A full entanglement monotone that is not convex, *Physical review letters* **95**, 090503 (2005).
- [40] K. Mølmer, Optical coherence: A convenient fiction, *Physical Review A* **55**, 3195 (1997).
- [41] A. Karnieli, N. Rivera, A. Arie, and I. Kaminer, The coherence of light is fundamentally tied to the quantum coherence of the emitting particle, *Science Advances* **7**, 10.1126/sciadv.abf8096 (2021).